

SOLAR SYSTEM ANALOGS AROUND *IRAS*-DISCOVERED DEBRIS DISKS

CHRISTINE H. CHEN¹, PATRICK SHEEHAN², DAN M. WATSON², P. MANOJ², AND JOAN R. NAJITA³

¹ Space Telescope Science Institute, 3700 San Martin Drive, Baltimore, MD 21218, USA; cchen@stsci.edu

² Department of Physics and Astronomy, University of Rochester, Rochester, NY 14627, USA

³ NOAO, 950 North Cherry Avenue, Tucson, AZ 85726, USA

Received 2009 April 22; accepted 2009 June 22; published 2009 July 31

ABSTRACT

We have rereduced *Spitzer* IRS spectra and reanalyzed the spectral energy distributions (SEDs) of three nearby debris disks: λ Boo, HD 139664, and HR 8799. We find that the thermal emission from these objects is well modeled using two single temperature black body components. For HR 8799—with no silicate emission features despite a relatively hot inner dust component ($T_{\text{gr}} = 150$ K)—we infer the presence of an asteroid belt interior to and a Kuiper Belt exterior to the recently discovered orbiting planets. For HD 139664, which has been imaged in scattered light, we infer the presence of strongly forward scattering grains, consistent with porous grains, if the cold, outer disk component generates both the observed scattered light and thermal emission. Finally, careful analysis of the λ Boo SED suggests that this system possesses a central clearing, indicating that selective accretion of solids onto the central star does not occur from a dusty disk.

Key words: circumstellar matter – planetary systems: formation

1. INTRODUCTION

Our solar system possesses four terrestrial planets, an asteroid belt, four Jovian planets, and a Kuiper Belt. Whether this planetary architecture is common or rare has not yet been quantified. Dusty disks, believed to be generated by collisions between parent bodies, analogous to asteroid and Kuiper Belt dust rings, have been detected around main-sequence stars via thermal infrared emission. Space-based mid- and far-infrared surveys indicate that $\sim 10\%$ – 30% of main-sequence stars possess infrared excess (Lagrange et al. 2000) and that 95% of these debris disks have color temperatures similar to that expected for cold dust in our Kuiper Belt (Meyer et al. 2007), suggesting that exo-Kuiper Belts are common around main-sequence stars. The remaining 5% of debris disks possess massive, warm, dusty disks that may be the result of planet formation in self-stirred disks (Kenyon & Bromley 2004) or massive, stochastic events such as the period of Late Heavy Bombardment in our solar system (Wyatt et al. 2007); however, whether lower mass, steady state, asteroid belts are common or rare is not yet known. At the current time, only the exo-asteroid belt around ζ Lep has been spatially resolved (Moerchen et al. 2007).

Warm, asteroidal dust may be more prevalent than currently inferred from broadband photometric surveys. High-resolution imaging suggests that some debris disks with cold spectral energy distribution (SED) color temperatures ($T_{\text{gr}} < 100$ K) may also possess warm components. Spatially resolved scattered light and thermal emission images of ~ 15 resolved debris disks reveal two distinct dust architectures: (1) continuous disks with surface density distributions that are well approximated by a combination of a rising and a decaying power law (e.g., β Pic, AU Mic) and (2) narrow belts with sharp inner edges (e.g., HR 4796A, Fomalhaut). Both geometries may possess dust at terrestrial temperatures. Ground-based mid-infrared imaging of β Pic detected an unresolved component of infrared excess originating from distances < 5 AU away from the central star (Telesco et al. 2005; Wahhaj et al. 2003) indicative of warm dust. Similar imaging of HR 4796A and Fomalhaut may also have detected unresolved warm dust components that are spatially distinct from the cold, narrow dust rings that are resolved

in scattered light and thermal emission (Koerner et al. 1998; Stapelfeldt et al. 2004).

Unfortunately, the majority of debris disks discovered thus far cannot currently be spatially resolved because their surface brightnesses are too faint or their angular sizes are too small. Additional techniques may shed light on the presence of warm dust in cold debris systems: (1) *Spitzer* 5.5–40 μm SED observations may reveal the presence of an additional component of warm dust (this study) and (2) nulling interferometry observations may reveal an unresolved dust component close to the star (Liu et al. 2004). We have been conducting a *Spitzer* IRS spectroscopic study of *IRAS*-discovered debris disks (Chen et al. 2006). Rereduction and reanalysis of our previously published observations finds four objects (λ Boo, HR 5825 (HD 139664), HR 8799) with warm dust in addition to the cold dust that was originally discovered using *IRAS*. The recent direct detection of three orbiting giant planets around HR 8799 (Marois et al. 2008) allows us to compare the planetary architecture of this system with that of our own. The synthesis of resolved scattered light images (Kalas et al. 2006) and the infrared SED allows us to place new constraints on the properties of dust grains around HD 139664.

2. OBSERVATIONS

The debris disks around the stars λ Boo, HR 5825 (HD 139664), and HR 8799 were first identified based on the presence of 60 μm *IRAS* excesses, 1–2 orders of magnitude brighter than expected from their stellar photospheres (Backman & Paresce 1993). Recent *Spitzer* MIPS 24 μm and 70 μm photometry has confirmed the presence of unresolved 24 μm and/or 70 μm excesses associated with λ Boo (Su et al. 2006) and HD 139664 (Beichman et al. 2006). The 7'' and 21'' angular resolutions of *Spitzer* at 24 and 70 μm , respectively, are a significant improvement from the 0.75×4.6 and 1.5×4.7 angular resolutions of *IRAS* at 25 and 60 μm , respectively, and better exclude confusion from the background and/or other nearby sources. Chen et al. (2006) measured the shape of the hot dust continuum emitted from these objects from low-resolution *Spitzer* IRS spectra and inferred the presence of warm dust with

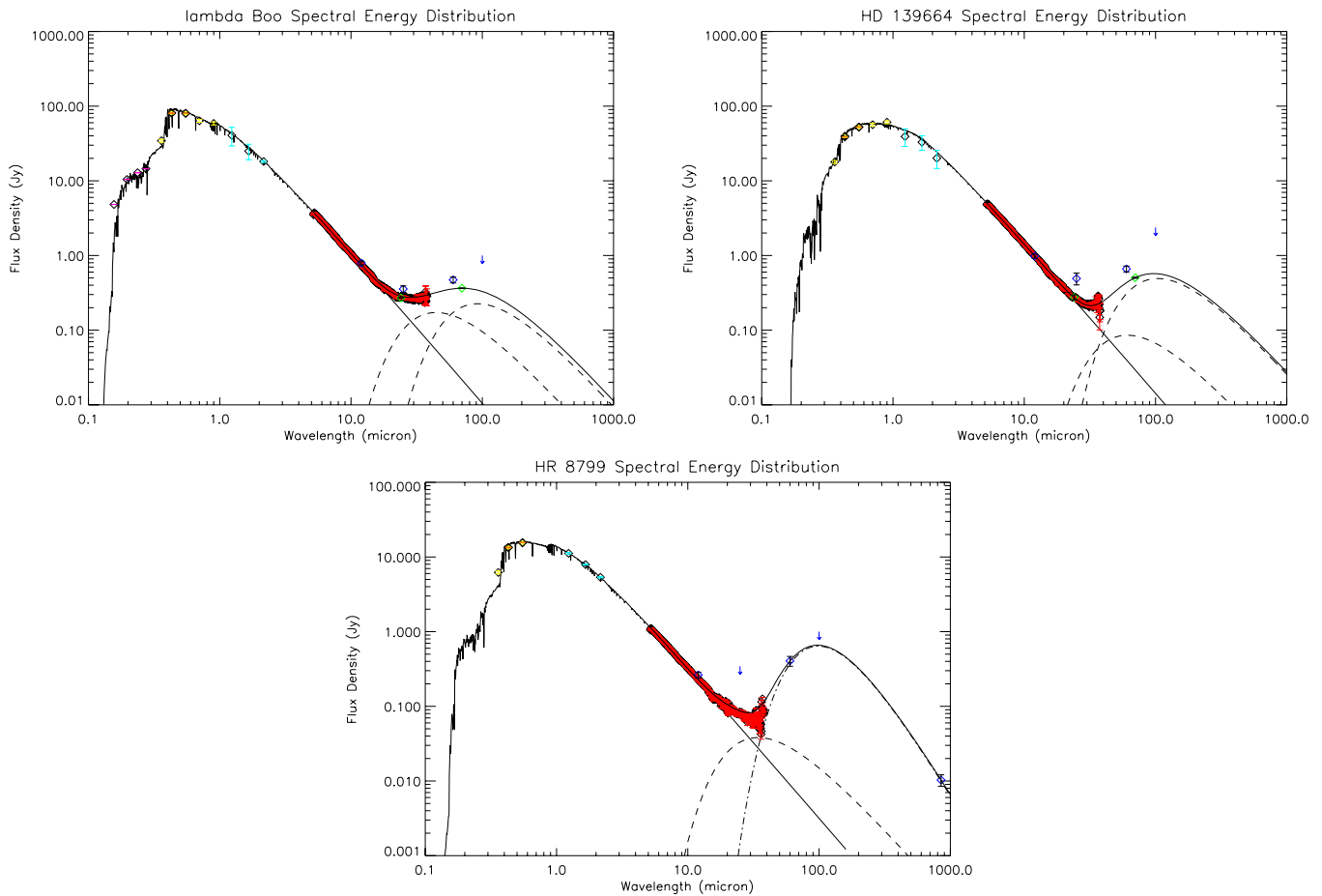


Figure 1. SEDs for λ Boo, HD 139664, and HR 8799: TD1 fluxes are plotted with magenta error bars; General Catalogue of Photometric Data mean UBV or Johnson et al. fluxes are plotted with yellow error bars; and 2MASS JHK fluxes are plotted with cyan error bars. Color-corrected IRS, MIPS, and *IRAS* data, where available, are shown with red, green, and blue error bars.

Table 1
Measured Fluxes

Name	Spectral Type	Distance (pc)	F_{ν} (8.5–13 μm) (mJy)	F_{ν} (30–34 μm) (mJy)
λ Boo	A0p	30	934 ± 5	258 ± 7
HD 139664	F5IV-V	18	1256 ± 7	211 ± 5
HR 8799	A5V	40	289 ± 3	65 ± 6

$T_{\text{gr}} = 100 \text{ K}–150 \text{ K}$, hotter than estimated from photometric observations alone.

We present updated IRS spectra, extracted from S15.3 pipeline products using the IRS team’s SMART program (Higdon et al. 2004), overlaid on Kurucz stellar photosphere models that are minimum χ^2 fit to TD1, Johnson UBVRI, and Two Micron All Sky Survey (2MASS) stellar photometry (where available) in Figure 1. Our new reduction improves the signal-to-noise ratio (S/N) of the spectra modestly and extends reliable continuum measurements to $38 \mu\text{m}$, beyond which second-order light decreases the S/N. In Table 1, we list the fluxes of our objects in two photometric bands that have been used to search for excess from silicates (8.5–13 μm) and cold grains (30–34 μm). The calibration uncertainty in the fluxes is $\sim 5\%$ and the measured statistical uncertainties are listed in Table 1. We fit the combined IRS, MIPS, and *IRAS* SEDs using two temperature black body models with the parameters listed in Table 2. We estimate the temperature of the warm component

by minimum χ^2 fitting the IRS excess at wavelengths shorter than $30 \mu\text{m}$ (Figure 2) and the temperature of the cool component by estimating the color temperature from the remaining 30–35 μm and *IRAS*-60 or MIPS-70 μm excesses. For HR 8799 with published submillimeter photometry (Williams & Andrews 2006), cold dust with an emissivity, $\kappa_{\nu} \propto \nu^{\beta}$ where $\beta = 1$, is needed to fit the far-infrared and submillimeter SED.

Direct imaging of HD 139664 and HR 8799 has provided additional information about their circumstellar environments. High contrast Keck and Gemini AO imaging has detected three planetary-mass objects orbiting HR 8799 with projected separations of 24, 38, and 68 AU and inferred masses 7, 10, and $10 M_{\text{Jup}}$, inferred from the measured *K*-band companion luminosities and the 60 Myr central star age (Marois et al. 2008). High contrast *Hubble Space Telescope* (HST) Advanced Camera for Surveys (ACS) scattered light imaging has resolved dust in an edge-on ring around HD 139664 with a possible inner edge at 60 AU, a dust peak at 83 AU, and a sharp outer boundary at 109 AU away from the central star (Kalas et al. 2006). Kalas et al. speculate on the presence of (1) planetary embryos forming at 83 AU that dynamically stir smaller parent bodies, producing a collisional cascade at this radius, (2) a planetary body either inside or outside of the disk that traps migrating dust grains into mean motion resonances, also producing a dusty ring, or (3) planetary bodies inside 60 AU and/or beyond 109 AU that confine dust into the narrow ring.

Table 2
Dust Properties

Name	Warm Dust					Cold Dust				
	β	T_{gr} (K)	D (AU)	L_{IR}/L_*	M_{PB} M_{\oplus}	β	T_{gr} (K)	D (AU)	L_{IR}/L_*	M_{PB} M_{\oplus}
λ Boo	0	110	27	5.8×10^{-6}	0.003	0	60	115	7.6×10^{-6}	0.004
HD 139664	0	80	21	4.2×10^{-6}	0.0004	0	50	61	2.4×10^{-5}	0.003
HR 8799	0	150	9	1.9×10^{-6}	0.0002	1	40	2000	2.5×10^{-5}	0.002

3. HR 8799

HR 8799 was known to possess a debris disk well before the three companions orbiting the central star were discovered. We examine the grain properties to elucidate the planetary system architecture.

We assume that the dust detected in this system via mid-to-far-infrared thermal emission is gravitationally bound to the system. In this case, we can estimate the minimum grain size by balancing the force due to radiation pressure with the force due to gravity. For small grains with radius, a , the force due to radiation pressure overcomes gravity for solid particles smaller than

$$a_{\text{min}} = \frac{3L_*}{8\pi G M_* c \rho}, \quad (1)$$

where L_* is the stellar luminosity. For HR 8799 with $L_* = 6.1 L_{\odot}$ and $M_* = 1.6 M_{\odot}$ (Chen et al. 2006), we estimate $a_{\text{min}} = 1.7$ and $4.7 \mu\text{m}$, assuming that the grains are either an amorphous carbon/silicate mixture or water ice (densities $\rho = 2.5$ and 0.91 g cm^{-3}), respectively. The 150 K temperature of the warm dust indicates that this population is unlikely to be composed of water ice. The sublimation lifetime of $4.7 \mu\text{m}$ water ice grains is expected to be

$$t_{\text{subl}} = \frac{a \rho T_{\text{gr}}^{1/2} e^{T_{\text{subl}}/T_{\text{gr}}}}{\dot{\sigma}_o} \quad (2)$$

(Jura et al. 1998), where $\dot{\sigma}_o$ is the mass rate per surface area ($=3.8 \times 10^8 \text{ g cm}^{-2} \text{ s}^{-1} \text{ K}^{1/2}$, $T_{\text{subl}} = 5530 \text{ K}$; Ford & Neufeld 2001). For HR 8799, we estimate that $4.7 \mu\text{m}$ solid-ice grains sublimate in 40 minutes. Analysis of the $10 \mu\text{m}$ and $20 \mu\text{m}$ silicate features emitted by T Tauri disks indicates that the warm dust in these systems is predominately composed of silicates (Sargent et al. 2006). However, silicate grains with $T_{\text{gr}} = 150 \text{ K}$, are expected to produce a strong $20 \mu\text{m}$ silicate emission feature that should be detected using IRS because the dust is optically thin. The lack of a $20 \mu\text{m}$ silicate emission feature may indicate that the warm grains may be significantly larger than the minimum grain size and can be modeled assuming that they are large, with emissivities that are constant as a function of wavelength. Another possible reason for the lack of silicate emission features is that the grains are composed of amorphous carbon. Amorphous carbon has a flat emissivity and therefore lacks spectral features. Disentangling the contribution of carbon to this grain composition is challenging. However, since the warm dust component of T Tauri disks is principally composed of silicates and icy bodies such as comets possess silicate emission features (Min et al. 2005), we believe that the composition in the HR 8799 disk is most likely silicate-rich rather than carbon-rich. The *IRAS* $60 \mu\text{m}$ and *SCUBA* $850 \mu\text{m}$ fluxes can only be modeled using grains with an emissivity that is inversely proportional to wavelength, suggesting that the cold grains are small ($a \ll \lambda/2\pi = 9.5 \mu\text{m}$), possibly below the sub-blow out size of $1 \mu\text{m}$.

Black bodies (with $2\pi a \gg \lambda$) in radiative equilibrium around a star with a luminosity, L_* , and grain temperature, T_{gr} , are expected to possess a distance, D , from the central star

$$T_{\text{gr}} = \left(\frac{L_*}{16\pi\sigma D^2} \right)^{1/4}. \quad (3)$$

For HR 8799 with $T_{\text{gr}}(\text{warm}) = 150 \text{ K}$, we estimate minimum grain distances $D_{\text{in}} = 8.7 \text{ AU}$, placing the warm dust well within the orbits of the three companions, analogous to asteroidal dust in our solar system. Small grains (with $2\pi a \ll \lambda$) in radiative equilibrium around a star with a luminosity, L_* , and grain temperature, T_{gr} , are expected to possess a distance, D , from the central star

$$T_{\text{gr}} = \left(\frac{L_* T_*}{16\pi\sigma D^2} \right)^{1/5}. \quad (4)$$

For HR 8799 with $T_{\text{gr}}(\text{cold}) = 40 \text{ K}$, we estimate minimum grain distances $D_{\text{out}} = 2000 \text{ AU}$, placing the cold dust well outside the orbits of the three companions, analogous to Kuiper Belt dust in our solar system. The warm dust temperature is higher than that of water ice sublimation, suggesting that the inner belt may possess rocky grains, while the cold dust temperature is not, suggesting that the outer belt may be icy.

At the current time, there are few detailed constraints on the orbits of each of the planetary-mass objects. To first order, the system appears face-on with circular orbits because the stellar $v \sin i$ ($=40 \text{ km s}^{-1}$) is statistically low for a late A-/early F-type star, the observed orbital motions for the b and c components are orthogonal to their position vectors (relative to the star) and have magnitudes that are commensurate with that expected for face-on circular orbits (Marois et al. 2008). Using the formalism of Chiang et al. (2009), we estimate that the chaotic zone associated with component b extends from 68 AU outward to $\sim 100 \text{ AU}$ and that of component d extends inward from 24 AU to 12 AU. The lack of detected dust at distances closer to the orbit of the innermost putative planet may suggest that either there are additional planets in this system that have not yet been detected or that the orbits of the detected planets are slightly eccentric, producing large regions in the disk where circumstellar grains might experience secular perturbations (Moro-Martín et al. 2007).

Reidemeister et al. (2009) have recently studied comprehensively the properties of the dust and planets around HR 8799, reaching many of the same conclusions; however, they assert that the HR 8799 IRS spectrum may show weak silicate emission and model the cold component using large grains. Their interpretation including a $10 \mu\text{m}$ silicate emission feature may arise from the presence of apparent absorption features in the low-resolution spectra at 8.5 and $15 \mu\text{m}$ that are probably artifacts from the edges of the SL2 and LL2 spectra.

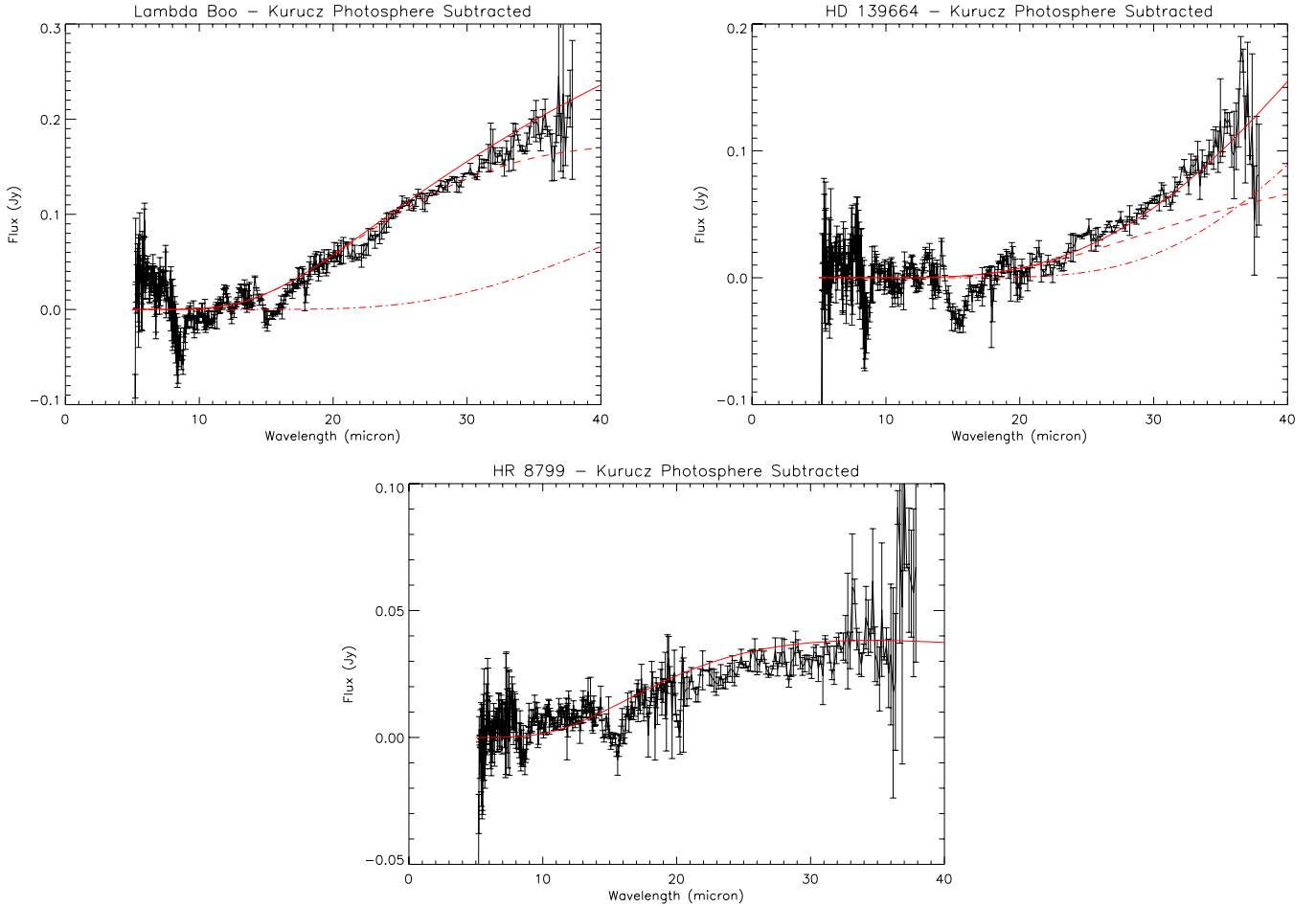


Figure 2. Photosphere-subtracted IRS spectra with F_v plotted as a function of wavelength. The minimum χ^2 fits for the two single temperature black body component are overlaid with the warm dust component shown as a dashed line, the cold dust component shown as a dashed-dotted line, and the sum of the two component as a solid line.

4. HD 139664

We can infer the dust architecture in the HD 139664 system assuming that the grains are large and well described by black bodies. For HD 139664 with $L_* = 3.6 L_\odot$ and $M_* = 2.7 M_\odot$ (Chen et al. 2006), we estimate $a_{\min} = 1.2 \mu\text{m}$ (assuming a grain density $\rho_s = 2.5 \text{ cm}^{-3}$). From our SED fit, we measure grain temperatures, $T_{\text{gr}}(\text{warm}) = 80 \text{ K}$ and $T_{\text{gr}}(\text{cold}) = 50 \text{ K}$, corresponding to minimum distances, $D_{\text{in}} = 21 \text{ AU}$ and $D_{\text{out}} = 61 \text{ AU}$. The similarity between the black body distance for the cold dust grains and the observed scattered light distance suggests that the thermal emission and scattered light are co-spatial, originating from the same grain population.

We can infer additional grain properties by comparing the scattered light and thermal emission from the cold dust population. We estimate a Bond albedo, $\omega = 0.3$, assuming $\omega\tau = 10^{-5}$ (Kalas et al. 2006) and $\tau = 3.6 \times 10^{-5}$ from our fit, higher than observed toward the zodiacal dust and the dust in the Fomalhaut disk ($\omega = 0.02$; Chiang et al. 2009) but similar to that of β Pic moving group member HD 181327 (Chen et al. 2008). We further estimate the ratio of the $0.6 \mu\text{m}$ scattering and $70 \mu\text{m}$ absorption coefficients. In our simple model, a single population of N grains with radius, a , emits a thermal flux,

$$F_v = \frac{\pi a^2}{d^2} N Q_{\text{abs}} B_v(T_{\text{gr}}), \quad (5)$$

where d ($=17.5 \text{ pc}$) is the distance from the observer to the

central star and Q_{abs} is the absorption coefficient. This same grain population is also expected to produce a scattered light surface brightness,

$$\text{SB} = \frac{L_{v,*}}{4\pi D^2} f(\theta) Q_{\text{sca}} \pi a^2 n, \quad (6)$$

where n is the grain column density, $f(\theta)$ is the scattering phase function for θ degrees of light deflection from forward scattering, and $L_{v,*}$ and Q_{sca} are the specific stellar luminosity and scattering coefficient at the scattered light wavelength observed ($0.5 \mu\text{m}$). We estimate the number of dust grains in the two ansa from the dust column density along our line of sight, n , assuming a projected area on the sky, $2\Delta r \Delta h$, where Δr and Δh are the measured radial width and the height of the ring, respectively. We derive the following constraint on the scattering and absorption coefficients,

$$\frac{Q_{\text{sca}}}{Q_{\text{abs}}} = \frac{D^2 B_v(T_{\text{gr}}) \text{SB}(\text{gr})}{d^4 F_{v,*} f(\pi/2) F_v(\text{gr})}. \quad (7)$$

For HD 139664 with $\Delta r \sim \Delta h \sim 83 \text{ AU}$, $\text{SB}(\text{gr}) = 11.0 \mu\text{Jy arcsec}^{-2}$ (Kalas et al. 2006) and $F_{v,*} = 52.6 \text{ Jy}$ at V band, $Q_{\text{sca}}(0.5 \mu\text{m})/Q_{\text{abs}}(70 \mu\text{m}) = 7.3 \times 10^{-4}/f(\pi/2)$. Typically, $Q_{\text{sca}}/Q_{\text{abs}}$ is of order unity for large grains, suggesting that the scattering phase function at 90° scattering, $f(\pi/2)$, must be very small. Assuming the Henyey–Greenstein phase function,

Table 3
Multiple Dust Belt Systems

HR	HD	Name	Spectral Type	Age (Myr)	D_{hot} (AU)	D_{cold} (AU)	References
1084	22049	ϵ Eri	K2V	850	~ 3	35–90	1
2020	39060	β Pic	A6V	12	< 5	100–1500	10, 11
3927	86087		A0V	50	~ 7	~ 50	2
4775	109085	η Crv	F2V	1000	~ 2	130–170	2, 12
4796	109573		A0V	8	< 20	60–87	5, 8
	113766		F3/F5V	16	~ 4	~ 30 –80	2
5351	125162	λ Boo	A0p	310	~ 24	~ 115	This work
	139664		F5IV-V	200	~ 15	60–110	4, this work
7329	181296	η Tel	A0Vn	12	~ 5	~ 30	2
8728	216956	Fomalhaut	A4V	200	< 10	130–160	3, 9
8799	218396		A5V	160	~ 8	~ 2000	7, this work

References. (1) Backman et al. 2009; (2) Chen et al. 2006; (3) Kalas et al. 2005; (4) Kalas et al. 2006; (5) Koerner et al. 1998; (6) Lisse et al. 2008; (7) Marois et al. 2008; (8) Schneider et al. 2009; (9) Stapelfeldt et al. 2004; (10) Telesco et al. 2005; (11) Wahhaj et al. 2003; (12) Wyatt et al. 2005.

we can rewrite the constraint on the scattering and absorption coefficients as a function of g , the asymmetric scattering parameter, $f(\pi/2) = (1 - g)^2/4\pi(1 + g)^{3/2}$ (Henyey & Greenstein 1941) and search for materials that satisfy this constraint. We calculate scattering and absorption coefficients and asymmetric scattering parameters using laboratory measurements of the optical constants for amorphous olivine (MgFeSiO₄; Dorschner et al. 1995) solid and fluffy grains (assuming a vacuum volume fraction of 0.9) using Bruggeman effective medium and Mie theory (Bohren & Huffman 1983). We find that large ($a > 40 \mu\text{m}$), porous olivine grains can satisfy our grain properties constraint while solid grains cannot. Large, porous grains have been used to explain the strong forward scattering and high polarization fraction observed in the AU Mic disk using *HST* ACS (Graham et al. 2007).

5. λ BOO

The star λ Boo has become the archetype of a class of Population I late B- to early F-type stars with moderate to extreme (up to a factor of 100) surface underabundances of Fe-peak elements and solar abundances of lighter elements (C, N, O, and S; Paunzen 2004). One possible hypothesis for the abundance anomalies seen toward λ Boo stars is that they selectively accrete material from their circumstellar environments. In this scenario, grains with icy mantles and refractory cores slowly spiral in under Poynting–Robertson drag, sublimating or photodesorbing water ice as they migrate inward. Once their volatile mantles have been depleted, their refractory cores are expelled via radiation pressure and the gas is accreted onto the star. This hypothesis predicts that λ Boo stars should possess debris disks with constant surface densities, governed by Poynting–Robertson drag, and SED’s with $F_{\nu} \propto \nu^{-1}$ (Jura et al. 1998). Preliminary SED analysis of six debris disks around A-type stars with IRS excess indicated the possibility that two λ Bootis stars (λ Boo and HR 1570) possessed disks with $F_{\nu} \propto \nu^{-1}$ and therefore uniform surface densities in contrast to debris disks around four normal A-type stars that possessed disks with cleared inner regions, better fit by single temperature black bodies (Jura et al. 2004). At the time, this observational result was consistent with the idea that the abundance anomalies of λ Boo stars might be generated by pollution of their stellar atmospheres via selective accretion of volatiles from inward migrating circumstellar dust grains. Since this result was published, more data have been obtained and

data reduction of spectra obtained early in the *Spitzer* mission has improved.

The connection between λ Boo stars and circumstellar and/or interstellar dust is highly uncertain today. Su et al. (2006) carried out a MIPS 24 and 70 μm survey searching for infrared excess associated with ~ 160 A-type stars, including 15 λ Boo stars (R. Gray’s λ Boo Web site: <http://www1.appstate.edu/dept/physics/spectrum/lambootxt>) with an average age of ~ 300 Myr. Their observations suggest that the 24 and 70 μm excess rate for λ Boo stars is higher than average, even though the average age for the aggregate sample is similar ~ 270 Myr. We estimate that 8/15 (53%) and 7/9 (78%) of the λ Boo stars possess 24 and 70 μm excesses, respectively, compared with 53/160 (33%) and 39/69 (57%) of the total sample, suggesting that the λ Boo phenomenon may be associated with circumstellar dust. Low-resolution IRS spectra of 6 λ Boo stars have been published thus far: HD 30422, HR 1570, HD 74873, HD 110411, λ Boo, and HD 183324. New models for the IRS spectra of HD 30422 and HD 110411 indicate that these objects are better fits using a power law, consistent with a uniform surface density disk with an inner radius coincident with the stellar radius (Morales et al. 2009); however, revised models for λ Boo and HR 1570 (Chen et al. 2006) spectra and newly published models for HD 74873 and HD 183324 (Morales et al. 2009) suggest that these objects are better fit using a black body, suggesting that the disks around these stars possess central clearings. Therefore, the mechanism by which grains material is selectively accreted may be diverse and may need to be revised. In any case, none of the objects presented here can be modeled using the selective accretion hypothesis because their SEDs are not well fitted assuming $F_{\nu} \propto \nu^{-1}$.

6. DISCUSSION

At the present time, a dozen systems are known to possess multiple dust belts, suggesting the presence of multiple parent body populations, perhaps analogous to the asteroid and Kuiper Belts in our solar system (see Table 3). These dusty bands apparently occur around stars with a wide range of spectral types and ages. Some are identified using SED modeling while others are discovered via high-resolution imaging. High-resolution imaging has discovered unresolved excesses (consistent with asteroidal dust) around objects whose SEDs are well fitted using a single cold dust population, indicating that multiple dust belts may be common in debris disks. The *Spitzer* Formation and Evolution of Planetary Systems (FEPSs) team surveyed 328 solar-like stars with ages 0.003–3 Gyr quantifying the evolution

of dust and gas around main-sequence stars using IRAC, IRS, and MIPS, finding that $\sim 10\%$ solar-like stars possess cold debris disks. Of the dusty disks, fully 1/3 are apparently better fit using multiple temperature components than single temperature black bodies (Hillenbrand et al. 2008), also suggesting that extended disks and multiple dust components may be common in debris disks.

The present-day asteroid and Kuiper Belts possess an estimated 0.0005 and $0.01 M_{\oplus}$ in large bodies, respectively, significantly smaller than originally inferred to exist in these regions ($\sim 2\text{--}3$ and $\sim 35 M_{\oplus}$, respectively). The migration of the outer planets and the subsequent crossing of the 2:1 resonance by Jupiter and Saturn is believed to have ejected or scattered the majority of the initial mass in the asteroid and Kuiper Belts (Levison et al. 2007). We estimate the mass for each debris belt observed toward λ Boo, HD 139664, and HR 8799 (see Table 3) assuming that the current mass in parent bodies is at least as large as the amount of dust that has been removed from the system thus far, $M_{PB} \geq 4 L_{IR} t_{age}/c^2$ (Chen & Jura 2001), assuming stellar ages, $t_{age} = 310, 300$ (Kalas et al. 2006), and 160 Myr (Marois et al. 2008), respectively. These estimates are lower bounds because radiation pressure (and not Poynting–Robertson drag) probably dominates the grain removal process. We find that (1) the minimum parent body masses in the warm and cold belts are $0.0002\text{--}0.003 M_{\oplus}$ and $0.002\text{--}0.004 M_{\oplus}$, respectively, similar to the present-day asteroid and Kuiper Belts and (2) the cold dust belts are $1\text{--}10\times$ more massive than the warm ones, suggesting that they have more similar masses than the present-day asteroid and Kuiper Belts.

7. CONCLUSIONS

We have rereduced the IRS spectra of three debris disks and reanalyzed their SEDs. We conclude the following:

1. The infrared SEDs of λ Boo, HD 139664, and HR 8799 are well fitted using two single temperature black bodies indicating the presence of two dust populations. For HR 8799, the warmer dust is interior to the newly discovered orbiting planets in an exo-zodiacal dust belt and the cooler dust is exterior to the planets in an exo-Kuiper Belt.
2. The cool grains in the HD 139664 must be strongly, forward scattering, consistent with large ($a > 40 \mu\text{m}$), porous grains if it produces both the thermal emission detected using *IRAS* and the scattered light disk resolved using *HST* ACS at visual wavelengths.
3. The debris disks around the majority of observed λ Boo stars apparently possess inner clearings similar to those around normal A-type stars, suggesting that simple dusty disks delivering grains from the outer regions of disks onto central stars are not responsible for the peculiar stellar abundances observed.

We thank J. Debes, M. Fitzgerald, W. Forrest, J. Graham, M. Jura, B. Macintosh, and J. Patience for their helpful comments and suggestions.

REFERENCES

- Backman, D. E., & Paresce, F. 1993, in *Protostars and Planets III*, ed. E. Levy & J. I. Lunine (Tucson, AZ: Univ. of Arizona Press), 1253
- Backman, D. E., et al. 2009, *ApJ*, **690**, 1522
- Beichman, C. A., et al. 2006, *ApJ*, **652**, 1674
- Bohren, C. F., & Huffman, D. R. 1983, *Absorption and Scattering of Light by Small Particles* (New York, NY: Wiley)
- Chen, C. H., Fitzgerald, M. P., & Smith, P. S. 2008, *ApJ*, **689**, 539
- Chen, C. H., & Jura, M. 2001, *ApJ*, **560**, L171
- Chen, C. H., et al. 2006, *ApJS*, **166**, 351
- Chiang, E., Kite, E., Kalas, P., Graham, J. R., & Clampin, M. 2009, *ApJ*, **693**, 734
- Dorschner, J., Begemann, B., Henning, Th., Jaeger, C., & Mutschke, H. 1995, *A&A*, **300**, 500
- Ford, K. E., & Neufeld, D. A. 2001, *ApJ*, **557**, L113
- Graham, J. R., Kalas, P., & Matthews, B. 2007, *ApJ*, **654**, 595
- Higdon, S. J. U., et al. 2004, *PASP*, **116**, 975
- Hillenbrand, L. A., et al. 2008, *ApJ*, **677**, 630
- Henry, L. G., & Greenstein, J. L. 1941, *ApJ*, **93**, 70
- Jura, M., et al. 2004, *ApJS*, **154**, 453
- Jura, M., Malkan, M., White, R., Telesco, C., Pina, R., & Fisher, R. S. 1998, *ApJ*, **505**, 897
- Kalas, P., Graham, J. R., & Clampin, M. C. 2005, *Nature*, **435**, 1067
- Kalas, P., Graham, J. R., Clampin, M. C., & Fitzgerald, M. P. 2006, *ApJ*, **637**, L57
- Kenyon, S. J., & Bromley, B. C. 2004, *AJ*, **127**, 513
- Koerner, D. W., Ressler, M. E., Werner, M. W., & Backman, D. E. 1998, *ApJ*, **503**, L83
- Lagrange, A.-M., Backman, D. E., & Artymowicz 2000, in *Protostars and Planets IV*, ed. V. Mannings, A. P. Boss, & S. S. Russell (Tucson, AZ: Univ. of Arizona Press), 639
- Levison, H. F., Morbidelli, A., Gomes, R., & Backman, D. 2007, in *Protostars and Planets V*, ed. B. Reipurth, D. Jewitt, & K. Keil (Tucson, AZ: Univ. of Arizona Press), 669
- Lisse, C. M., Chen, C. H., Wyatt, M. C., & Morlok, A. 2008, *ApJ*, **673**, 1106
- Liu, W. M., et al. 2004, *ApJ*, **610**, L125
- Marois, C., Macintosh, B., Barman, T., Zuckerman, B., Song, I., Patience, J., Lafreniere, D., & Doyon, R. 2008, *Science*, **322**, 1348
- Meyer, M. R., Backman, D. E., Weinberger, A. J., & Wyatt, M. C. 2007, in *Protostars and Planets V*, ed. B. Reipurth, D. Jewitt, & K. Keil (Tucson, AZ: Univ. of Arizona Press), 573
- Min, M., Hovenier, J. W., de Koter, A., Waters, L. B. F. M., & Dominik, C. 2005, *Icarus*, **179**, 158
- Moerchen, M. M., Telesco, C. M., Packham, C., & Kehoe, T. J. J. 2007, *ApJ*, **655**, L109
- Morales, F. Y., et al. 2009, *ApJ*, **699**, 1067
- Moro-Martín, A., et al. 2007, *ApJ*, **668**, 1165
- Paunzen, E. 2004, in *The A-Star Puzzle*, ed. J. Zverko, et al. (Cambridge: Cambridge Univ. Press), 443
- Reidemeister, M., Krivov, A. V., Schmidt, T. O. B., Fiedler, S., Müller, S., Löhne, T., & Neuhäuser, R. 2009, *Icarus*, in press
- Sargent, B., et al. 2006, *ApJ*, **645**, 395
- Schneider, G., Weinberger, A. J., Becklin, E. E., Debes, J. H., & Smith, B. A. 2009, *AJ*, **137**, 53
- Stapelfeldt, K. R., et al. 2004, *ApJS*, **154**, 458
- Su, K. Y. L., et al. 2006, *ApJ*, **653**, 675
- Telesco, C. T., et al. 2005, *Nature*, **433**, 133
- Wahhaj, Z., Koerner, D. W., Ressler, M. E., Werner, M. W., Backman, D. E., & Sargent, A. I. 2003, *ApJ*, **584**, L27
- Williams, J. P., & Andrews, S. M. 2006, *ApJ*, **653**, 1480
- Wyatt, M. C., Greaves, J. S., Dent, W. R. F., & Coulson, I. M. 2005, *ApJ*, **620**, 492
- Wyatt, M. C., Smith, R., Greaves, J. S., Beichman, C. A., Bryden, G., & Lisse, C. M. 2007, *ApJ*, **658**, 569